Behaviour of Rectangular Hollow Steel Beams Strengthened with CFRP Sheets Applied in Longitudinal and Transversal Directions

Hanan Hussien Eltobgy, Anwar Badawy Abu-Sena, Omer Nazmi Abdelnabi

Abstract — Carbon Fibers Reinforced Polymers (CFRP) are widely utilized to strengthening various structural elements in order to sustain higher loads or to restore the strength of the deteriorated elements. This paper aims to investigate the behavior of hollow steel beams reinforced by unidirectional carbon fibers composite laminates applied in longitudinal and transversal directions. Experimental and numerical investigations were conducted in this study. Six specimens of rectangular hollow sectional (RHS) were subjected to a four-point loading test and divided into two groups. Each group of three specimens was tested in different positions "Mx and My". Each group included one reference beam and two, specimens strengthened with CFRP laminates in longitudinal and transversal directions. Ultimate loads and deflection were determined through the tests. Numerical analysis was performed using a finite element program in order to determine the failure load of beams. Results of finite element model were verified with their experimental counterparts, it is found in a good agreement. As per experimental results, using the CFRP strengthening system effectively improved the strength and the ductility of strengthened beams. Also, strengthened beams with longitudinal laminates achieved a higher improvement compared to strengthened beams with transversal laminates.

Index Terms— Rectangular Hollow Steel Section, CFRP, Strengthening, Stiffness, Strength, Pucks' failure criteria

1. INTRODUCTION

Hollow steel sections (HSS) are widely utilized in various structural systems, aiming to achieve the designer goals with the lowest cost. Hollow sectional shape inherits a superior properties compared to other sectional shapes which qualify hollow steel sections (HSS) to sustain a higher loads with the thinner steel thickness, and accordingly achieve more profits by saving steel material. On the other hand, thinner thickness of steel plates rises for the buckling tendency and losing a considerable portion of strength steel section, especially for elements exposed to corrosion. So, CFRP applications have a great importance to restore the strength of corroded steel hollow sections or to enhance its behaviour to sustain higher loads. This importance has attracted many researchers to investigate CFRP application with hollow steel section.

Photiou et al. [1] experimentally investigated the effectiveness of an ultra-high modulus, and a high modulus, CFRP in strengthening an artificially degraded steel beam of rectangular cross-section under four-point loading. Four beams were strengthened with hybrid lay-up of CFRP and glass fiber reinforced polymer (GFRP) bonded to bottom flange, two utilizing U-shaped units, which extended up the vertical sides of the beam to the neutral axis height, whereas the other two beams used a flat plate. The composite containing the ultra-high modulus CFRP failed when the ultimate strain of the carbon fiber was reached in the pure moment region. The failure load exceeded the plastic collapse load of the undamaged beam, thus demonstrating the effectiveness of the proposed upgrading scheme. The beams using the high modulus CFRP reached even higher ultimate loads and exhibited ductile response leading to very high deflections; neither fiber breakage nor adhesive failure was observed in either the U-shaped or the flat plate strengthened beam.

Also, Elchalakani et al. [2] presents experimental investigations for two series of CFRP strengthened and rehabilitated model box girders under quasi-static large deformation 3-point bending. The first series represented strengthening 12 un-degraded rectangular hollow section (RHS) beams from the manufacturer using externally wrapped CFRP sheets. The second series included rehabilitation of 41 artificially degraded RHS beams strengthened using externally wrapped sheets or bonded plates. The main parameters examined in this paper were the section type, section and member slenderness and the type and number of the CFRP sheets. The CFRP sheets were wrapped around the section in the transverse direction. The results show that the combined flexural and bearing strength of the steel box girder can be significantly increased by adhesively bonding CFRP. The average gain in strength due to bonding the CFRP laminate was 65% and 19.9% for the strengthening and rehabilitations series, respectively. The percent increase in strength was mostly affected by the section slenderness where the maximum gain was obtained for the slender section.

Moreover, CFRP strengthened hollow steel column subjected to lateral impact load were investigated by references [3, 4 and 5], using experimentally and

- *Associate Professor of Steel Structures, Civil Engineering Department, Faculty of Engineering at Shoubra, Benha University, Email: hanan.altobgy@feng.bu.edu.eg*
- *Professor of Steel Structures, Civil Engineering Department, Faculty of Engineering at Shoubra, Benha University, Email: A.Badawy@feng.bu.edu.eg*
- *Assistant Lecturer, Civil Engineering Department, Faculty of Engineering at Shoubra, Benha University, Cairo, Egypt, Email: omer.nazmi@feng.bu.edu.eg*

numerical investigations utilized techniques improved the impact resistance capacity of strengthened column.

As per available literature, many of parameters have not been covered well such as; applying longitudinal wrapping techniques covering all over the rectangular hollow section, Also, behaviour of CFRP strengthened hollow steel section subjected to pure bending moment. Therefore, this study aims to complete missing items in this topic by studying the behaviour of CFRP strengthened hollow steel section and subjected to pure bending moments about major and minor axes. Six specimens were subjected to four-points loading test. The specimens were divided to two group; first group was subjected to bending about major axes while second group was subjected to bending about minor axis. Each group has three specimens, first specimen is a bare beam while the rest of them were strengthened with a single laminate of CFRP applied either on longitudinal direction or transversal direction.

2. EXPERIMENTAL PROGRAM

2.1 Specimen dimensions

Experimental scheme was designed to evaluate the impact of using carbon reinforced fiber polymer sheets to strengthen hollow steel section subjected to major and minor bending moment. Six specimens were selected as shown on Table 1. Two groups of hollow steel beams were selected to achieve the variation on aspect ratio. Group G1 was subjected to bending moment about major axis, while group G2 with shallow depth was subjected to bending about minor axis. Using wide plates with a relatively large slenderness ratio increases buckling tendency of steel plates. Slender status of sectional plates are calculated by comparing to width to thickness ratios limits presented at table 4.1b, AISC360-16 [6] using averaged yield stresses obtained from the coupon tests conducted in this study.

Figure 1 illustrates schematic for CFRP wrapping techniques applied on steel beams. Two wrapping techniques of CFRP sheets were utilized in this study. Term “FRP -1L” refers to steel specimen wrapped with a single layer of CFRP applied on longitudinal direction. Term “FRP -1T” refers to steel specimen wrapped with a single layer of CFRP applied on transversal direction. While term “NOFRP” refers to control specimen without any wrapping.

2.2 Material properties

Steel properties were determined from the results of tensile coupon tests. Four coupons were prepared as shown in figure 2. Coupon tests were performed using the universal testing machine, Galdabini-Quasar 600. Table 2 summarizes steel properties determined from the coupon tests.

Carbon fiber fabrics “Sika Wrap ®-230C” and epoxy resin “Sika dur®-330” were used as a composite strengthening system. Table 3 shows the properties of Sika Wrap®-230C and Sikadur-330 obtained from the manufacturer data sheets, [7 and 8].

TABLE 1. SPECIMENS PROPERTIES.

Group no.	Section size Depth* Width*Th. d * b * t	Aspect ratio b/d	Slenderness ratio		Specimens ID
			d/t	b/t	
G1	RHS 150*50*1.8	1/3	80.3 (N.C.)	24.7 (C.)	B11-150-50-NOFRP
					B12-150-50-FRP-1L
					B13-150-50-FRP-1T
G2	RHS 50*150*1.8	3	24.7 (C.)	80.3 (S.)	B16-50-150-NOFRP
					B17-50-150-FRP-1L
					B18-50-150-FRP-1T

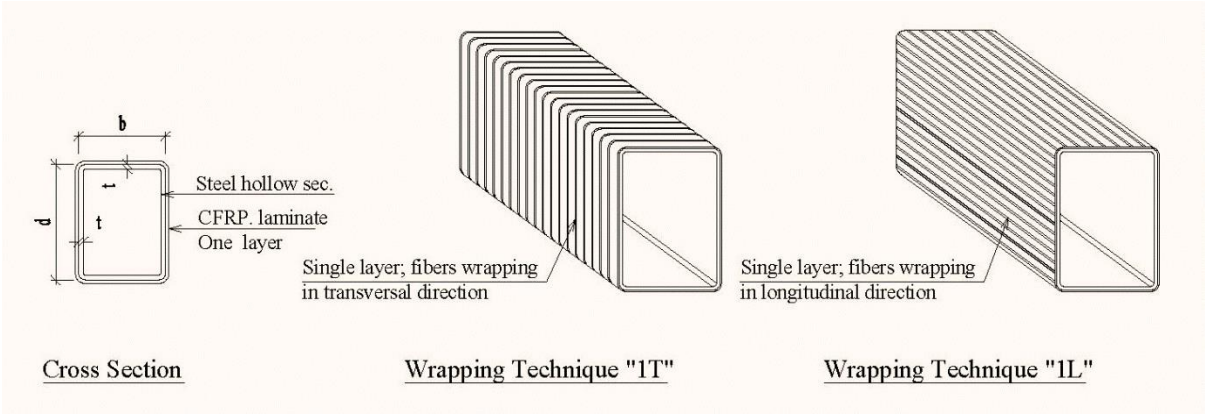

FIGURE 1. SCHEMATIC VIEW FOR STRENGTHENING TECHNIQUES, 1L & 1T.

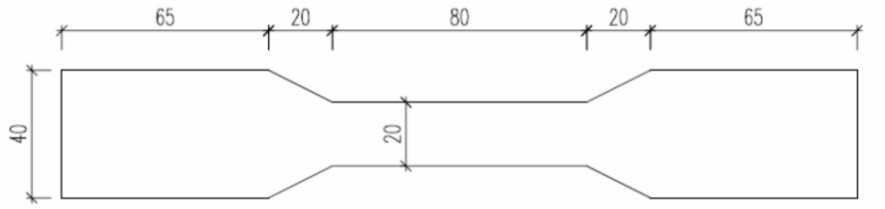

FIGURE 2. SPECIMEN DIMENSION OF COUPON TESTS.

TABLE 2; COUPON TESTS' RESULTS.

Coupon tests ID	Thickness t (mm)		Yield stress Fy (Mpa)		Ultimate stress Fu (Mpa)		Ultimate elongation eu (%)
		AVR.		AVR.		AVR.	
T7	1.81	1.8	333	322	379	374	25.3
T8	1.79		314		370		23.4
T9	1.81		314		373		23.4
T10	1.8		328		375		25.3

TABLE 3.A. PRODUCT INFORMATION OF WOVEN UNIDIRECTIONAL CARBON FIBER FABRIC, SIKA WRAP® - 230 C.

Fiber type	mid-range strength carbon fibers
Area Density	235 g/m2 ±10 g/m2
Dry fibers thickness	0.129 mm
Dry fibers density	1.82 g/cm3
Tensile strength of fibers	4 000 N/mm2
Tensile modulus of fibers	230 000 N/mm2
Elongation at break	1.7 %
Fabric length/roll	50 m
Fabric width	300 mm -600 mm
Shelf life	24 months from date of production

TABLE 3.B. TECHNICAL DATA OF EPOXY IMPREGNATION RESIN, SIKA DUR®-330.

Composition	epoxy resin
Packaging	two components (A+B)
Mix ratio	A:B = 4:1
Density	1.30 ± 0.1 kg/l
Application temperature	+10 °C min. / +35 °C max
Tensile strength	33.8 N/mm2
Compressive strength	80 N/mm2
Flexural elastic modulus	3489 N/mm2
Elongation at break	1.2 %
Shelf life	24 months from date of production

TABLE 3.C. TECHNICAL DATA OF CFRP OF SIKA WRAP® - 230 C., CHARACTERISTIC PROPERTIES BASED ON ASTM D 3039

Laminate nominal thickness	0.129 mm
Laminate nominal cross section	129 mm2 per m width
Laminate tensile strength	3200 kN/mm2
Laminate tensile modulus of elasticity	210 kN/mm2
Laminate elongation at break	1.59 %

FIGURE 3. PROCESS OF PREPARING STEEL SURFACE USING SAND PAPER.

2.3 Specimen Preparation

The final surface of steel must be smooth, dry and free of rusts and any other contaminants as dust, foreign particles, oil, grease and surface coatings, etc. which could adversely affect or inhibit the bond of the strengthening system to the steel. Surface of steel specimens prepared well for applying CFRP laminate by mechanical processing using a rotary wire brush and sandpapers in additional to final chemical cleaning by thinner-based solvent. Figure 3 shows surface perpetration process of steel beams using a rotary sandpaper.

For the dry application of the Sika Wrap®-230C system, Sika dur®-330 is normally used for the resin priming coat and as the impregnating resin. The resins were mixed and spread onto the prepared surfaces according to manufacturer instructions. Then, Carbon fiber fabrics were wrapped onto the adhesive coat according to orientation specified for each specimen. All specimens were left for two weeks to achieve excellent bond between steel and CFRP, [7 and 8].

2.4 Testing method

All specimens had 1900 mm clear span, and subjected to four-point bending tests. Experimental tests were performed by using hydraulic jack, hydraulic pump, and loading cell of 500 KN capacity. Spreader beam was used to transfer applied load in two separated position over the specimen. Pure bending moment induced internally at the middle region of beam. Also, bearing plates and stiffener plates were provided for specimens to eliminate stress concentrations. Figures 4 and 5 show the configurations of four-points loading test utilized for bare steel and strengthened beams, respectively.

Linear voltage displacement transducers (LVDT) were used to determine beam deflections at three positions, at the positions of applying loads and at the middle of the beam. Also, Strain gages were attached to CFRP laminates in order to monitor the shortening and the elongation induced in the carbon fibers. Figure 6 shows the different positions of strain gages fastened to CFRP laminates at the mid-span of beam.

During the testing procedure, data logger system recorded several measurements collecting them from connected instruments, loading cell, LVDTs and strain gauges. Specimens were subjected to vertical load with small increments till failure occurs. Also, failure behavior accompanying to ultimate load was noticed for each specimen.

2.5 Experimental results and discussion.

Table 4.a shows the ultimate vertical loads and corresponding deflections for all test specimens. Also, specimen's deflections corresponding to ultimate loads of relative bare beam are presented. In addition, maximum strains for CFRP laminates are shown in Table 4.b., +ve value refer to elongation in the CFRP.

Ultimate loads and deflections.

Figures 7. a and b show load - deflection curves of the tested specimens of group G1 and G2, respectively. The plotted curves illustrate the behavior of specimens during loading tests, and show the ultimate loads for the strengthening techniques. It can be noticed that all curves tend to decrease by approaching of ultimate loads, which indicates to buckling occurrence leads to reduction in beam stiffness. On the other hand, the curve declination of CFRP strengthened beam was less pronounced. This is attributed to wrapping with CFRP that succeeded in constraining the buckling deformations and thus improving the strength.

All strengthened specimens achieved a significant improvement in the ultimate load and deflection compared to corresponding results of bare steel beams. Improvement percentage of ultimate loads for specimens B12-1L, B13-1T, B17-1L and B18-1T are 13%, 14%, 28% and 17% respectively, and the improvement percentage of corresponding deflections are 29%, 23%, 36% and 23% respectively.

Ultimate loads and Failure modes

Figure 13 shows the failure mode for specimen, B12-1L as an example of specimens of group G1. Specimens of group G1 failed under a flexural failure mode combined between the web crippling phenomena. Web crippling phenomena occurred at loading regions resulted from loading application over beam flange. While, specimens of group G2 subjected to flange buckling mode, which attributed to high tendency for buckling resulted from using slender flange plate.

Furthermore, physical damages of CFRP laminates were observed at loaded regions contributing with whole failure mode. Also, slippage failure between CFRP sheets and steel surface wasn't observed during all specimens tests.

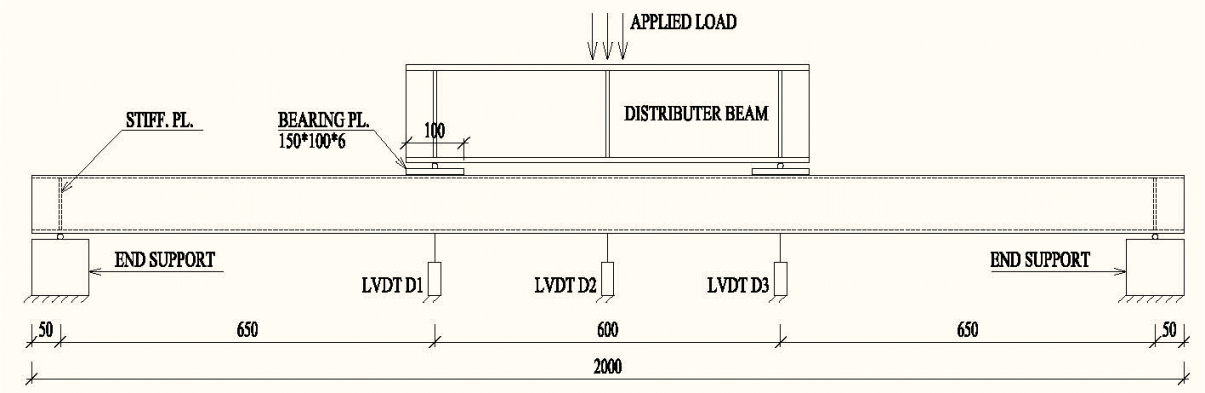

FIGURE 4 CONFIGURATION OF BENDING TEST FOR BARE BEAMS.

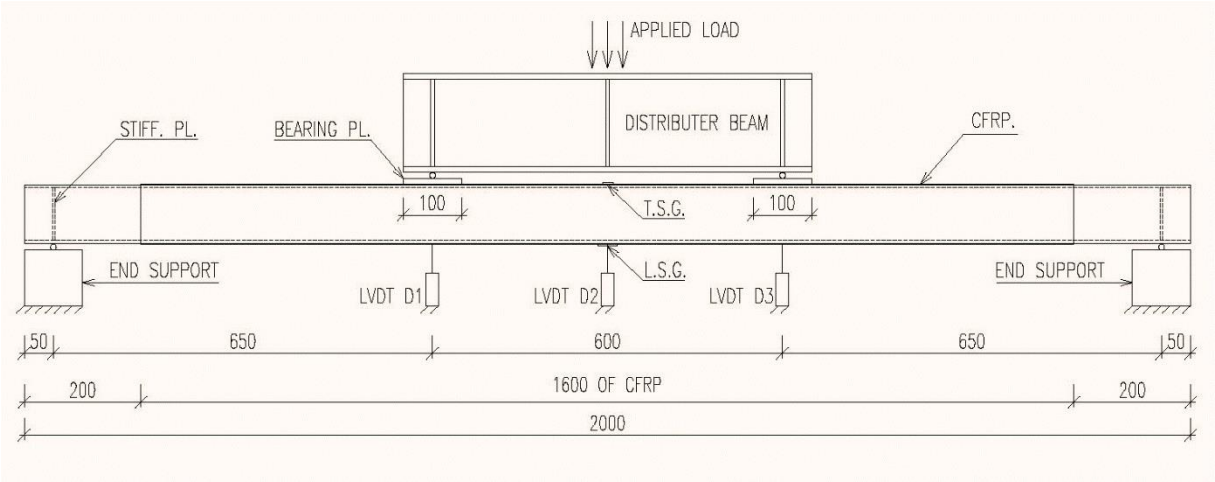

FIGURE 5 CONFIGURATION OF BENDING TEST FOR STRENGTHENED BEAMS.

A). ATTACHED TO LOWER FLANGE IN CASE OF LONGITUDINAL CFRP LAMINATES.

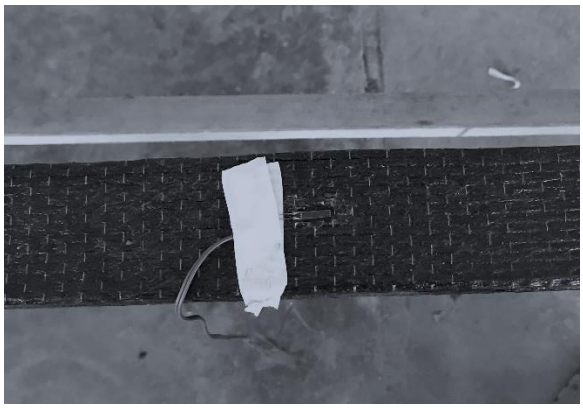

B) ATTACHED TO TOP FLANGE IN CASE OF TRANSVERSAL CFRP LAMINATES.

FIGURE 6. SAMPLES OF STRAIN GAGES ATTACHED TO CFRP LAMINATES AT MID-SPAN OF BEAM

Table 4.a. Experimental results: ultimate loads and deflections.

Group no.	Specimens ID	Ultimate load (kN.)	Ultimate load ratio	Deflection at failure (mm)	Corresponding deflection (mm)	Corresponding deflection ratio
G1	B11-150-50-NOFRP	24.08	1.00	11.35	11.35	1.00
	B12-150-50-FRP-1L	27.10	1.13	10.50	8.04	0.71
	B13-150-50-FRP-1T	27.39	1.14	10.57	8.70	0.77
G2	B16-50-150-NOFRP	8.35	1.00	21.80	21.80	1.00
	B17-50-150-FRP-1L	10.68	1.28	28.10	13.95	0.64
	B18-50-150-FRP-1T	9.75	1.17	25.80	16.86	0.77

Table 4.b. Experimental results: recorded strains.

Group no.	Specimens ID	Max. Strain for CFRP layer
G1	B12-150-50-FRP-1L	+1881 *10^{-6}
	B13-150-50-FRP-1T	+407 *10^{-6}
G2	B17-50-150-FRP-1L	+930 *10^{-6}
	B18-50-150-FRP-1T	+1821 *10^{-6}

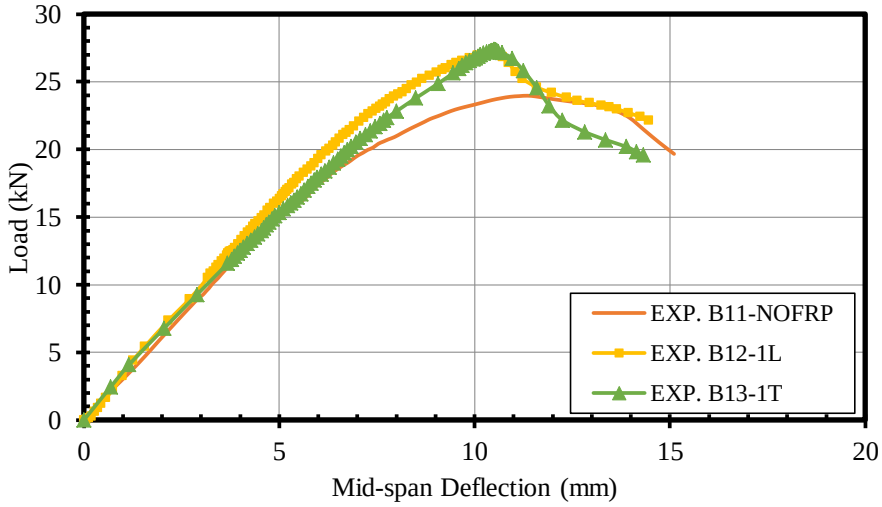

FIGURE 7.A. LOAD VERSUS DEFLECTION CURVES FOR SPECIMENS' GROUP G1

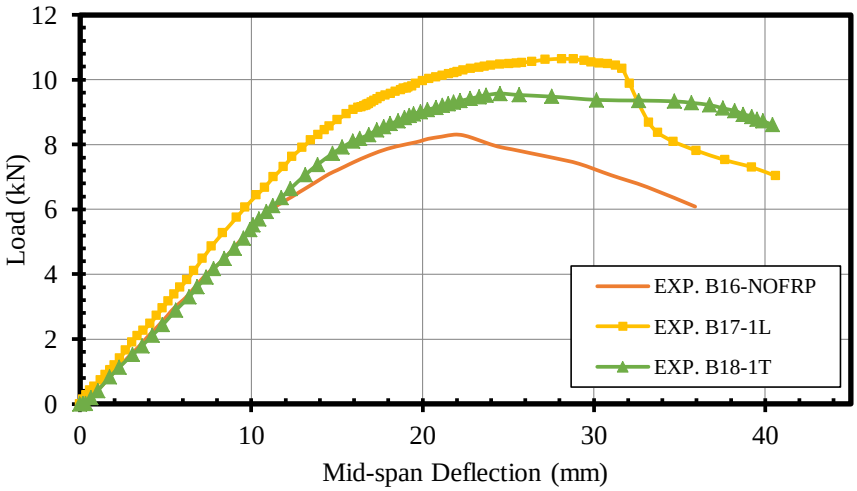

FIGURE 7.B. LOAD VERSUS DEFLECTION CURVES FOR SPECIMENS' GROUP G2

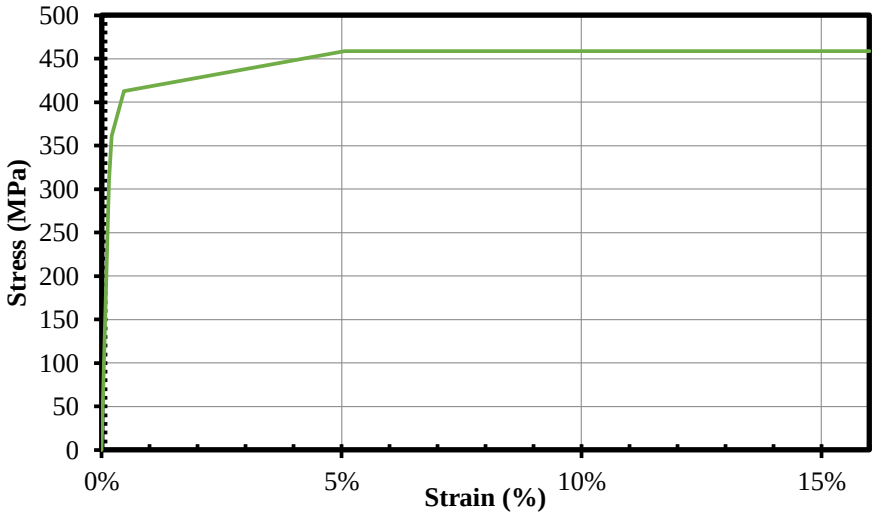

FIGURE 8. IDEALIZED STRESS-STRAIN CURVES FOR COUPON TESTS.

3. FINITE ELEMENT ANALYSIS MODEL

Tested specimens were simulated using commercial program, ANSYS 17.2 [9]. Finite element model was developed to investigate the behavior of CFRP strengthened hollow steel section and subjected to uniform bending moment. Eigen value and non-linear analyses were utilized in the investigation. The finite element models results were compared with the experimental results in order to verify the accuracy of developed model

Analysis models were developed based on the dimensions of tested specimens, presented at table 1, adopting the configuration of four-points loading test shown in figure 5.

3.1 Material Modeling

Figure 8 shows stress-strain curve for coupon tests used to define steel material in the numerical model. Steel was simulated in the finite element model as a multi-linear isotropic hardening material. Stress-strain curve is based on cold formed steel model proposed by Abdel-Rahman and Sivakumaran [10].

In this idealized model, the elastic stress-strain behaviour is represented by a linear segment with a slope equals to the modulus of elasticity (E) up to a proportional strength limit (F_p), which is equivalent to the initial yielding point of the material. The gradual yielding behaviour can be idealized using a bi-linear representation (with tangent moduli E_{T1} and E_{T2}) between the proportional limit (F_p) and the yield strength (F_y) passing through an intermediate yielding strength (F_{ym}). This intermediate strength (F_{ym}) is taken as the half-way point strength between (F_p) and (F_y). The strain hardening behaviour is next represented by a linear segment with a tangent moduli (E_{T3}).The proposed values for the tangent moduli (E_{T1}, E_{T2}, and E_{T3}) are 100,000 MPa, 20,000 MPa, and 1,000 MPa, [10]. Idealized stress-strain curves for coupon tests were defined using average values of yield and ultimate stresses resulted from coupon tests shown in table 2. While, young's modulus (E) and Poisson's ratio (□□) were taken equal to 205,000 Mpa and 0.3 respectively.

CFRP composite is made up of unidirectional carbon fibers that have been saturated in polymers as shown in figure 6. When compared to polymers, carbon fibers offer a higher stiffness and strength. Like a result, each plan has various properties, and CFRP composite behaves as an orthotropic material. While the properties of transversal planes perpendicular to the longitudinal direction of fibers are nearly identical, CFRP composite can be thought of as a specific case of orthotropic material, dubbed transversally isotropic.

In this study, composite properties of carbon fibers and adhesive resin were adopted for the simulation of CFRP laminate, Batuwitage et al. [11]. CFRP laminate was simulated as a transversally isotropic linear elastic material using the mechanical properties defined at table 3.b & c.

Properties at longitudinal direction are based on the technical information of CFRP laminates provided at manufacturer data sheets of Sika Wrap ®-230C, [7] these properties were predetermined to consider the variable thickness between nominal dry carbon fibers and effective primer coat. Compressive strength in x-direction was taken equal to 78% of tensile strength recommended by research findings presented by Mostofinejad et al. [12] and practical ratios presented by ECP 208 [13].

Properties at Y and Z directions are based on the technical information of adhesive resin provided at

manufacturer data sheets for Sika dur®-330, [8]. While, shear strengths were taken equal 80% of tensile resin strength as recommended by research conclusions/results presented by Xia et al. [14] & Fernando et al. [16].

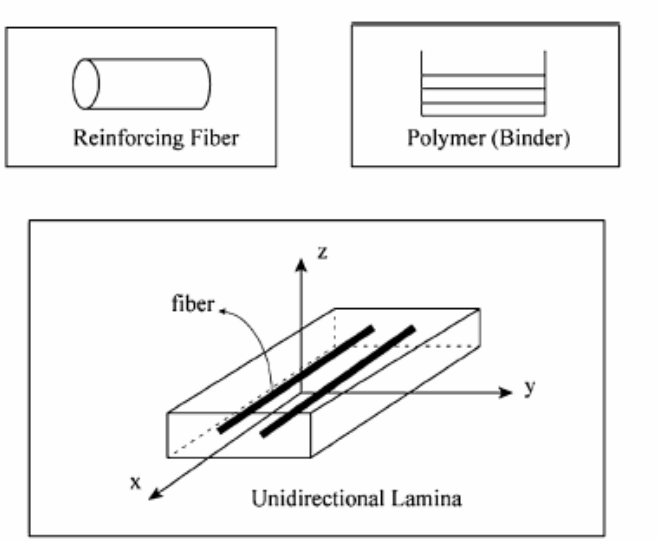

FIGURE 9. SCHEMATIC OF FRP COMPOSITE Kachlakev et al. [15].

In this study, Pucks' failure criteria, [17] and a progressive damage model were utilized to simulate post-failure behavior of CFRP laminate. Pucks' failure criteria are used to determine the onset of failure for CFRP composite. It has well-established criteria for evaluating fiber and inter-fiber failure modes [18], as well as a high degree of accuracy when compared to other approaches [19]. The maximum stresses resulting from the critical orientation angle of the fracture planes can be considered in inter-fiber failure (IFF) modes. Where, the progressive damage model is capable of describing the post-failure behavior of CFRP laminate by decreasing the material stiffness immediately once failure occurred.

3.2 Element Types and Mesh

Test specimens were simulated as a three-dimensional finite element model using the 2D shell element "Shell 181" [20 and 21]. Shell 181 is a four-node shell element with six degrees of freedom at each node. Plasticity, huge deflections, and large strains can all be described using "Shell 181". Fine mesh with a maximum size of 10mmx10mm was used in the modelling of flange, web, and curved plates to obtain acceptable accuracy. Figure 10 displays the finite element mesh for RHS 150*50*1.5 as an example.

Shell section of "Shell 181" can be defined as multilayer, with variable characteristics defining each layer. Multilayer definition was used to simulate strengthened walls using varied characteristics for steel and CFRP laminates. The material characteristics, layer thickness, and layer orientation were specified. However, full contact between layers was considered and slippage was not permitted, bond failure behaviour was compensated by inter-lamination failure, which was based on Puck's failure criterion. All specimens were modelled as a simply supported beam matching with experimental configuration. Figure 11 displays orientation definition of shell layers on F.E. in order to define various cases of wrapping techniques.

3.3 Analyses Types

In this study, eigenvalue analysis and nonlinear analyses were used. To obtain the buckling shape of the critical mode, eigen value analysis was used, which was then scaled to imitate the initial geometrical flaw. Maximum observed bows for groups G1 and G2 attached to sectional depth are 0.75mm, according to measured dimensions for steel sections. The maximum amplitude of the initial defect was calculated using the measured values.

On the finite element model, nonlinear material, progressive damage evolution, and large displacement were adopted. Also, in order to determine collapse loads, analyses were carried out using the arc-length method as an incremental load control.

3.4 Finite Element Validation

Load displacement curves and failure mode shapes were used to validate the finite element models against the experimental tests. Figure 12 compares load-deflection curves derived from finite element analysis and those obtained from experimental tests. The curves show that the results are in good agreement.

Figures 13 compares between the deformed shapes and failures modes obtained from the finite element analysis and the experimental tests for specimen, B12-L1. Internal steel stress was plotted on the deformed shape of finite element model which indicates that reaching the failure was combined by buckling occurrence. Also, failed regions of CFRP laminate, 1L, predicted by Puck's failure criteria and degradation model are shown in figures 13.d and e aside with the experimental test. Comparisons show a good similarity between relative deformed shapes and failures modes. Also, failed regions of CFRP laminates predicted by finite element model are in a good agreements with physical damaged regions observed in experimental tests.

According to the comparisons results, the finite element model can be used to predict the behaviour and strength of steel hollow beams reinforced with CFRP.

4. CONCLUSIONS

This paper experimentally investigated the structural behaviour of hollow steel beam strengthened by CFRP laminates in longitudinal and transversal direction. Six specimens were subjected to four points loading test up

to failure loads. Tested specimens were subjected to bending moments about the major and the minor axes. A finite element model was developed to simulate CFRP

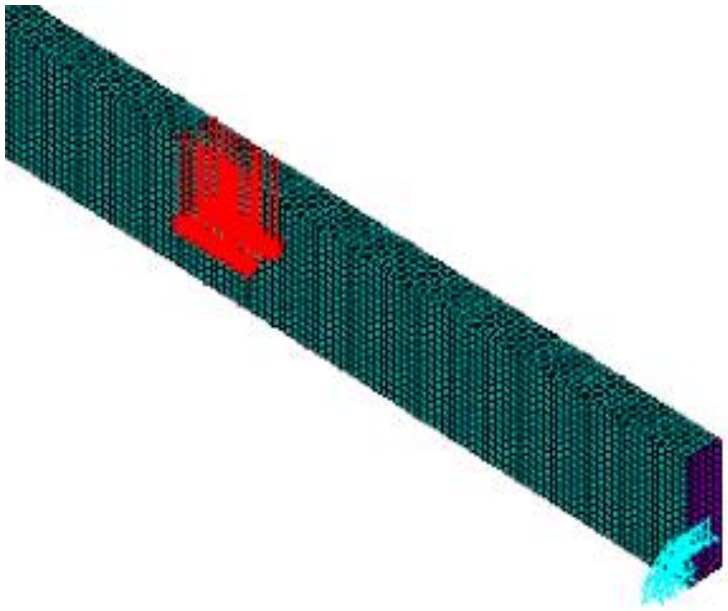

FIGURE 10. HALF VIEW OF 3D- F.E. MODEL FOR SHS150*50*1.8 AS AN EXAMPLE

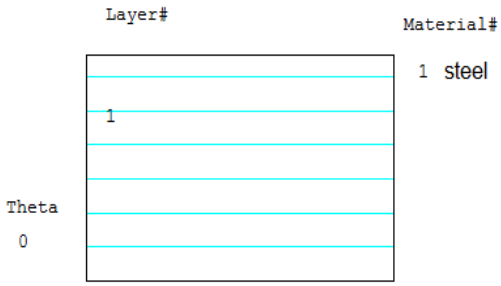

FIGURE 11.A. ORIENTATION DEFINITION FOR SINGLE LAYER FOR STEEL PLATES WITHOUT ANY WRAPPING.

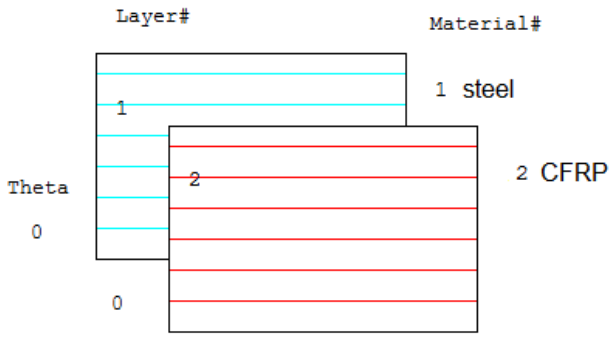

FIGURE 11.B. ORIENTATION DEFINITION STEEL LAYER FOLLOWED BY CFRP LAYER (1L).

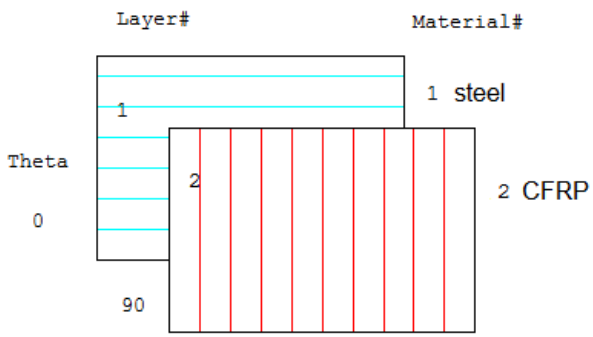

FIGURE 11.C. ORIENTATION DEFINITION STEEL LAYER FOLLOWED BY CFRP LAYER (1T).

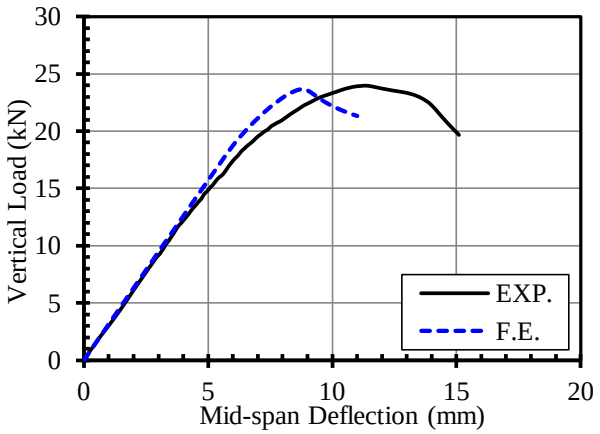

For Specimen B11

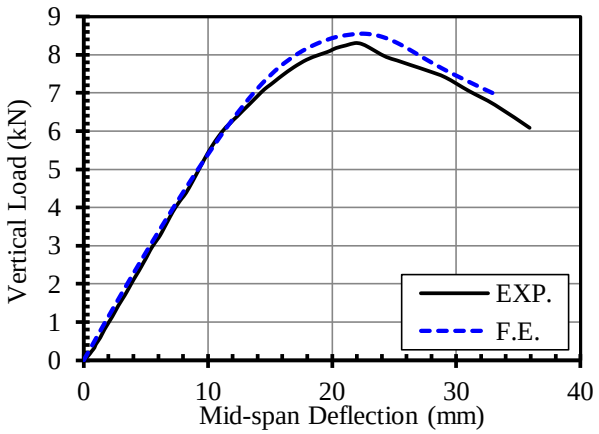

For Specimen B16

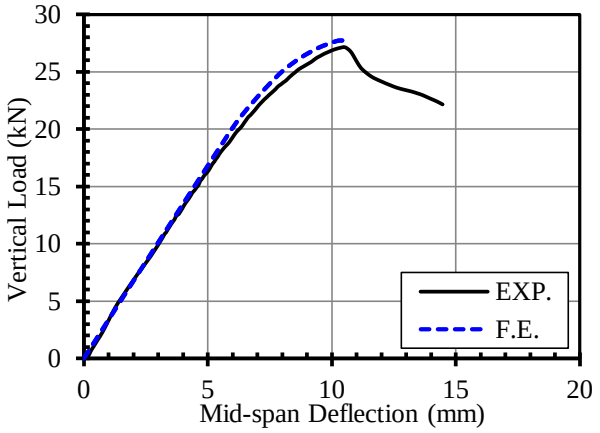

For Specimen B12

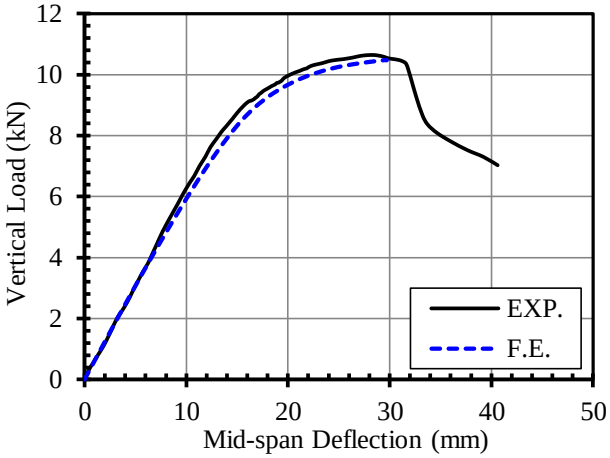

For Specimen B17

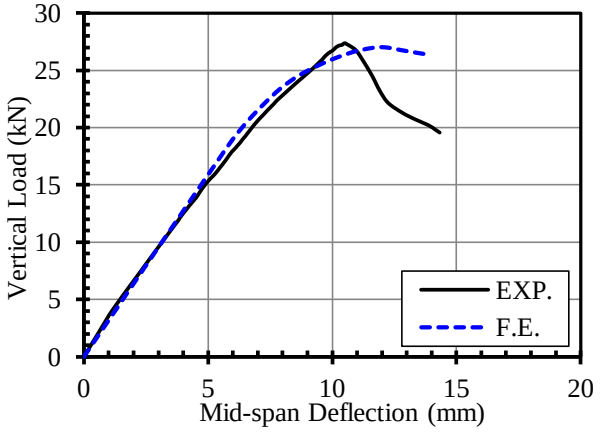

For Specimen B13

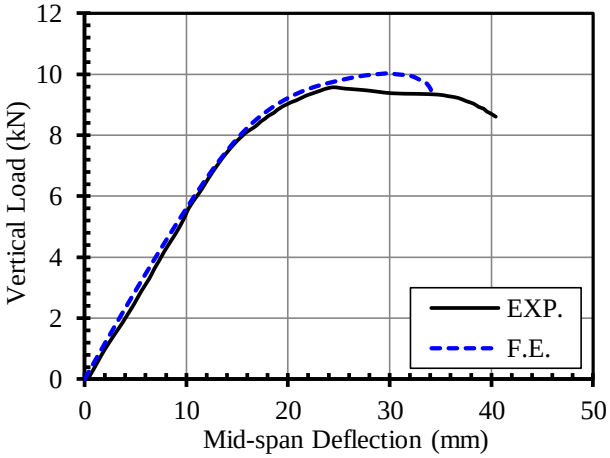

Specimen B18

FIGURE 12. VERTICAL LOAD – MID-SPAN DEFLECTION CURVES OF THE TESTED SPECIMENS

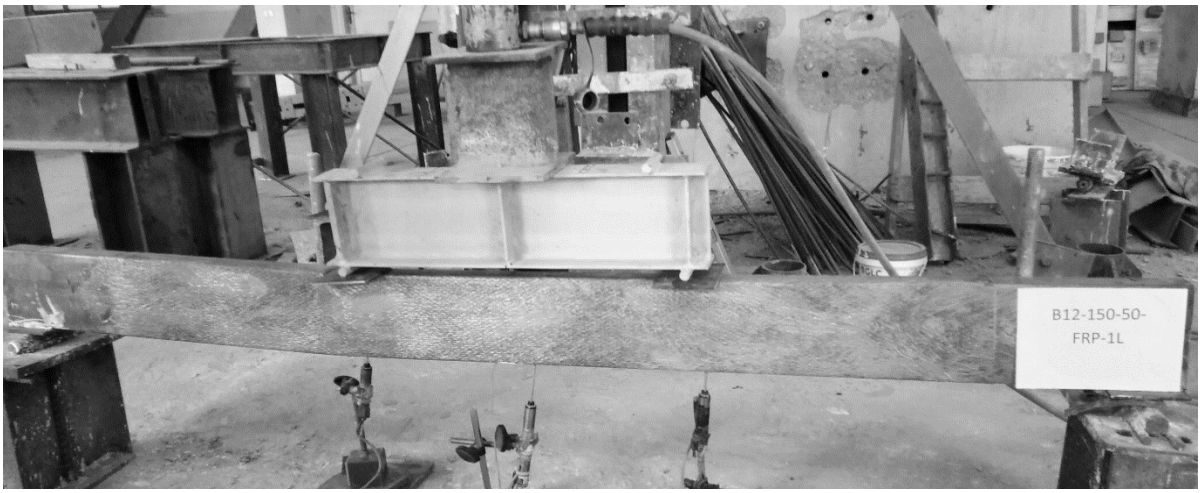

A.) OVERALL PICTURE OF SPECIMEN B12-1L DURING FAILURE

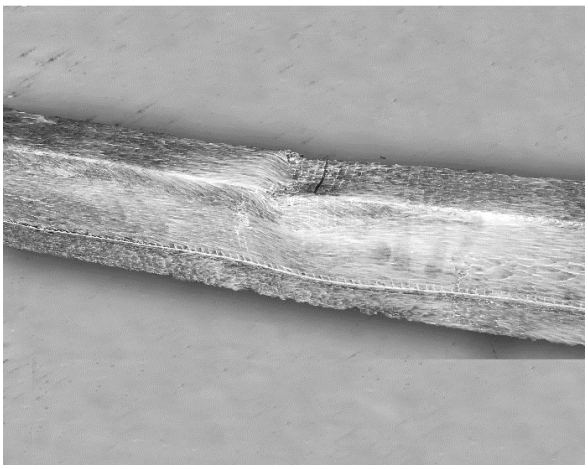

B.) EXPERIMENTAL FAILURE

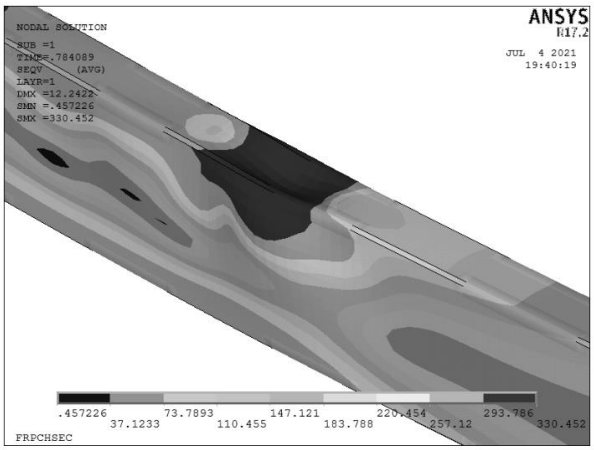

C.) F.E. DEFORMATIONS WITH STEEL STRESSES.

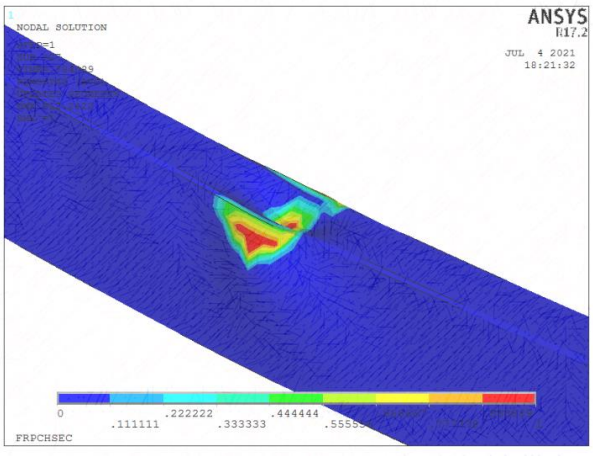

D.) CONTOURED DEGRADATION OF FAILED LAMINATE,1L

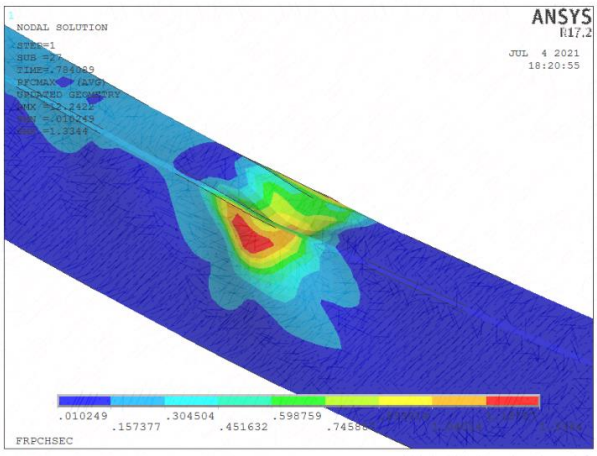

E.) CONTOURED PUCK'S STRESS FACTOR OF LAMINATE, 1L.

FIGURE 13. COMPARISON BETWEEN DEFORMATIONS OF SPECIMEN B12-1L OBTAINED FROM TESTS AND F.E.

Strengthened beams using ANSYS program. Puck's failure criteria and progressive damaged model were adopted to simulate failure behaviour of CFRP laminate. The results of F.E. model were verified by the experimental results. According to the experimental results, all strengthened specimens achieved greater strength compared to strength of control specimens. The main findings of this study can be noted as follows; The developed model using finite element program ANSYS accurately simulates the behavior of CFRP strengthened hollow steel beams and accurately predicts the capacities and deflection. Adopted Puck's failure criteria in the finite element model can effectively calculate fiber and inter-fiber failure modes of CFRP laminates and properly determine the initiation of laminates damage. Adopted progressive damaged model in the finite element model can effectively decrease the stiffness of failed CFRP laminates and properly simulates the post-failure behavior of CFRP laminates.All utilized CFRP wrapping techniques effectively enhanced the ultimate capacity and the deflection of hollow steel section subjected to four points loadings test compared to the results of bare steel beams, regardless the axis of loading application. CFRP Strengthening technique "1L" where sheets were wrapped in longitudinal directions achieved the outmost improvments for the ultimate load and deflection of strengthened beams compared to CFRP Strengthening techniques "1T where sheets were wrapped in transversal directions and vice versa.

References

[1]. Photiou N.K, Hollaway L.C, and Chryssanthopoulos M.K. "Strengthening of an artificially degraded steel beam utilizing a carbon/glass composite system" Construction and Building Materials 20 (2006) 11–21

[2]. Elchalakani M. "CFRP Strengthening and Rehabilitation of Degraded Steel Welded RHS Beams Under Combined Bending and Bearing" Thin-Walled Structures 77 (2014) 86–108.

[3]. Yu Chena, Jun Wana, Kang He " Experimental Investigation on Axial Compressive Strength Of Lateral Impact Damaged Short Steel Columns Repaired With CFRP Sheets" Thin-Walled Structures 131 (2018) 531–546.

[4]. Md Iftekharul Alam, Sabrina Fawzia "Numerical Studies on CFRP Strengthened Steel Columns Under Transverse Impact" Composite Structures 120 (2015) 428–441.

[5]. Majid M.A. Kadhim, Zhangjian Wu, Lee S. Cunningham "Loading Rate Effects On CFRP Strengthened Steel Square Hollow Sections Under Lateral Impact" Engineering Structures 171 (2018) 874–882.

[6]. American Institute of Steel Construction (AISC). Manual of Steel Construction. Chicago, Illinois, USA: Load and Resistance Factor Design (LRFD); March 2016

[7]. SIKA EGYPT Company ''Sika Wrap®-230C. Product data sheet" March 2020, Version 01.03.

[8]. SIKA EGYPT Company ''Sika dur®-330. Product data sheet" August 2018, Version 01.01.

[9]. ANSYS, Finite Element Analysis Program and Theory Manuals, Release V17.2, 2016.

[10]. Abdel-Rahman N, and Sivakumaran K.S. "Evaluation and Modeling of the Material Properties for Analysis of Cold-Formed Steel Sections" International Specialty Conference on Cold-Formed Steel Structures. Paper 3, October 17, 1996.

[11]. Batuwitage C, Fawzia S, Thambiratnam DP, Tafsirojjaman T, Al-Mahaidi R, and Elchalakani M. "CFRP-Wrapped Hollow Steel Tubes Under Axial Impact Loading." Tubular Struct. XVI Proc. 16th Int. Symp. Tubul. Struct. (ISTS 2017, 4-6 December 2017, Melbourne, Aust., CRC Press; 2017, p. 401-407.

[12]. Mostofinejad D, and Moshiri N. "Compressive strength of CFRP composites used for strengthening of RC columns: comparative evaluation of EBR and grooving methods." J. Compos. Constr. 2015; 19 (5).

[13]. ECP Committee 208-05 "Egyptian code of practice for the use of fiber reinforced polymer in the construction field" ECP Committee 208, Ministry of Housing and Urban Communities, Egypt, 2005.

[14]. Xia S.H, and Teng J.G. "Behaviour of FRP-to-Steel Bonded Joints" the International Symposium on Bond Behaviour of FRP in Structures (BBFS 2005).

[15]. Kachlakev D, Miller T, Yim S, Chansawat K, and Potisuk T. "Finite element modeling of reinforced concrete structures strengthened with FRP laminates". Final Report SPR-316, Oregon Department of Transportation, May 2001.

[16]. Fernando D, Yu T, and Teng T.G. "Behavior and Modeling of CFRP-Strengthened Rectangular Steel Tubes Subjected to a Transverse End Bearing Load" International Journal of Structural Stability and Dynamics Vol. 15, No. 8 (2015) 1540031 (24 pages).

[17]. Puck A, Kopp J, and Knops M. "Guidelines for the Determination of the Parameters in Puck's Action Plane Strength Criterion" Composites Science and Technology. Vol. 62.371-378. 2002.

[18]. Gu J, Li K, and Su L. "A Continuum Damage Model for Intralaminar Progressive Failure Analysis of CFRP Laminates" Materials 2019, 12, 3292

[19]. Bright R.J, and Sumathi M. "Failure Analysis of FRP Composite Laminates Using Progressive Failure Criteria" International Journal of Scientific & Engineering Research Volume 8, Issue 6, June-2017.

[20]. Kumar A, and Rangavittal H.K. "Convergence Studies in the Finite Element Analysis of CFRP Shaft under Torsion Using Shell281, Shell181, and Comparison with Analytical Results." In: Li C., Chandrasekhar U., Onwubolu G. (eds) Advances in Engineering Design and Simulation, (2020), Lecture Notes on Multidisciplinary Industrial Engineering. Springer, Singapore. https://doi.org/10.1007/978-981-13-8468-4_17.

[21]. Barour S, and Zergua A. "Finite Element Modeling of Strengthened Beams Using CFRP" J. Build. Mater. Struct. (2019) 6: 77-87, DOI: 10.5281/zenodo.3352308.